A noticeable increase (by 0.012) in the isotropic part g_{av} is observed for the diselenolene complex. A similar situation has been found for the bis(dialkyldichalcogenocarbamato)copper(II) complexes $Cu(R_2dsc)_2$ and $Cu(R_2dtc)_2$, which represent another $CuS_4/CuSe_4$ couple. Also in this case the **g** tensor becomes more rhombic and its principal axes do not coincide with those of A^{Cu} on going from the CuS_4 to the $CuSe_4$ complex. According to detailed MO calculations[13,20] made on these systems, the increased **g** anisotropy in the coordination plane (see Table I) is mainly due to the large spin-orbit coupling of the Se donor atoms (the spin-orbit coupling constant of Se is λ_{Se} = 1690 cm^{-1}, which is larger than that of Cu by a factor of 2), giving rise to enhanced ligand orbital contributions of different weight (mainly Se $4p_z$ orbits of an antibonding state) to the corresponding **g** components. Of course delocalization reduces the effect of the Cu spin-orbit contribution to the **g** tensor, but apparently the spin-orbit contribution of the Se atoms more than compensate for this. However, for the $Cu(R_2dsc)_2$ complexes, instead of an increase, a decrease of g_{av} by about 0.025 was found. Since the covalency of the Cu-Se bonds in $[Cu(dsit)_2]^{2-}$ comes close to that observed for the copper diselenocarbamates, this can only be understood if for $[Cu(dsit)_2]^{2-}$ the d-d excitation energies of the MO's that contribute to the principal **g** values are smaller than those of $Cu(R_2dsc)_2$. Unfortunately, in the electronic spectrum of $[Cu(dsit)_2]^{2-}$, an unambiguous assignment of the transitions observed cannot be made, and detailed MO calculations, which could clarify the situation, require also the knowledge of exact X-ray structural data for the Cu complex, which are not available.

The noncoincidence of the principal axes can only be observed if the symmetry of the complex is lower than rhombic symmetry. Furthermore, MO calculations on diselenocarbamates have shown that also the 4d Se ortibals have to be included in the calculations to account for the noncoincidence of the **g** and **A** tensors.[13,20]

Acknowledgment. We wish to express our thanks to Prof. Dr. E. de Boer (University of Nijmegen) for his continual interest and critical reading of the manuscript.

(20) Keijzers, C. P.; de Boer, E. *Mol. Phys.* **1975**, *29*, 1743.

Contribution from the Department of Chemistry and Center for Micro-Engineered Ceramics, University of New Mexico, Albuquerque, New Mexico 87131, and Department of Chemistry, University of Delaware, Newark, Delaware 19716

Synthesis and Characterization of Alkali-Metal Titanium Alkoxide Compounds $MTi(O\text{-}i\text{-}Pr)_5$ (M = Li, Na, K): Single-Crystal X-ray Diffraction Structure of $[LiTi(O\text{-}i\text{-}Pr)_5]_2$

M. J. Hampden-Smith,*,† D. S. Williams,† and A. L. Rheingold‡

Received March 20, 1990

The series $[MTi(O\text{-}i\text{-}Pr)_5]$, M = Li, Na, or K, has been prepared by the reaction of MO-*i*-Pr with $Ti(O\text{-}i\text{-}Pr)_4$. A single-crystal X-ray diffraction study revealed that $[LiTi(O\text{-}i\text{-}Pr)_5]$ crystallizes from toluene at -30 °C in the monoclinic space group $P2_1/n$, with unit cell dimensions a = 11.440 (8) Å, b = 16.396 (13) Å, c = 11.838 (8) Å, β = 92.59 (5)°, and Z = 4, as a dimer containing two approximately trigonal-bipyramidal titanium centers linked by lithium bridges. In benzene solution, all three compounds are dimeric, as revealed by cryoscopic molecular weight determination, and all three undergo an alkoxide ligand exchange process that is rapid on the ^1H NMR time scale at room temperature. The positions of ν(M-O) are assigned based on the low-energy shifts observed upon deuteriation of the isopropoxide ligands.

Introduction

The use of metal alkoxides as molecular precursors for electronic and ceramic materials is an area of intense current interest and has recently been reviewed.[1] The sol-gel technique for hydrolytic condensation has been used for many years as a low-temperature method for conversion of metal alkoxides to metal oxides.[2] For example, hydrolysis of mixtures of $[Sr(O\text{-}i\text{-}Pr)_2]$ with $[Ti(O\text{-}i\text{-}Pr)_4]$ or $[Zr(O\text{-}i\text{-}Pr)_4]$, followed by calcination at 350 °C, resulted in formation of crystalline perovskite phases, $SrTiO_3$ and $SrZrO_3$.[3] Another advantage of the sol-gel process lies in control over homogeneity on the molecular level. Although there are many examples of the use of this technique for the synthesis of ternary metal oxide phases[1,2] and many examples of mixed-metal alkoxide compounds in the literature,[4] there is very little structure information available. Perhaps the best characterized series of mixed-metal alkoxides is $MSn(O\text{-}t\text{-}Bu)_3$ in which M has been systematically varied (M = Li, Na, K, Rb, Cs, Tl), revealing some interesting trends.[5] Whereas M = Li and Na derivatives are dimeric, with a common $Sn_6O_6M_2$ cage as a structural feature, M = K, Rb, and Cs derivatives exist as one-dimensional infinite polymers with a common SnO_3M cage, and the M = Tl derivative exists as a monomer in the solid state. These trends have been examined in a recent review article.[6] A notable feature of the structure of the $LiMSn(O\text{-}t\text{-}Bu)_3$ (M = Li, Na) analogues is the coordination environment of the alkali-metal ions,

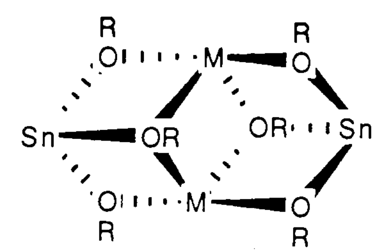

which could be described as distorted octahedral with two cis

* Author to whom correspondence should be addressed.
† University of New Mexico.
‡ University of Delaware.

(1) Bradley, D. C. *Chem. Rev.* **1989**, *89*, 1317. Hubert-Pfalzgraf, L. G. *New. J. Chem.* **1987**, *11*, 663.
(2) (a) Klemperer, W. G.; Mainz, V. V.; Ramanurthi, S. D.; Rosenburg, F. S. In *Better Ceramics Through Chemistry III*; Brinker, C. J., Clark, D. E., Ulrich, D. R., Eds.; North Holland: New York, 1988. (b) Riman, R. E.; Haaland, D. M.; Northrup, C. J. M.; Bowen, H. K.; Bleier, A. *Mater. Res. Soc. Symp. Proc.* **1984**, *32*, 233. (c) Fukushima, J.; Kodaira, K.; Matsushita, T. *Am. Ceram. Soc. Bull.* **1976**, *55*, 1064. (d) Kirbir, F.; Komiyama, H. *Chem. Lett.* **1988**, 791. (e) Shiota, M. *J. Mater. Sci.* **1988**, *23*, 1718. (f) Bradley, D. C.; Holloway, H. *Can. J. Chem.* **1962**, *40*, 1176. (g) Rousset, A.; Chassagneux, F.; Paris, J. *J. Mater. Sci.* **1986**, *21*, 3111. (h) Hench, L. L., Ulrich, D. R., Eds. *Ultrastructure Processing of Ceramics, Glasses and Composites*; John Wiley and Sons: New York, 1984. (i) Goel, S. C.; Kramer, K. S.; Gibbons, P. C.; Buhro, W. E. *Inorg. Chem.* **1989**, *28*, 3619. (j) Matchett, M. A.; Chiang, M. Y.; Buhro, W. E. *Inorg. Chem.* **1990**, *29*, 358.
(3) Smith, J. S.; Dolloff, R. T.; Mazdiyasni, K. S. *J. Am. Cer. Soc.* **1970**, *53*, 91.

0020-1669/90/1329-4076$02.50/0

vacancies. A similar coordination environment for Na was also observed in NaCe$_2$(O-*t*-Bu)$_9$.[7]

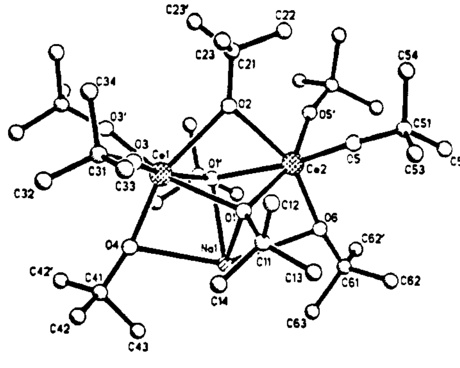

We have also recently characterized the species [Tl$_2$Sn(OEt)$_6$], which is a one-dimensional polymer in the solid state, but which is monomeric in solution.[8]

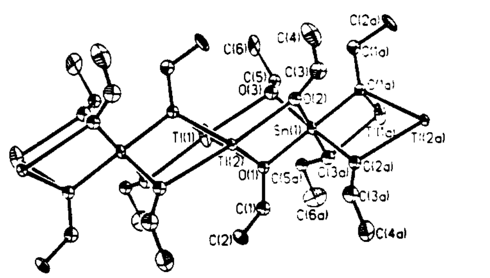

In this species, the thallium ions exist in a similar coordination environment, and the general molecular architecture is similar to that of **1**. The different degrees of oligomerization observed for [Tl$_2$Sn(OEt)$_6$] in the solid state and in solution emphasizes the need for both solid-state *and* solution structural characterization of these species, especially since hydrolytic condensation is performed in the liquid phase. In this work, we report the synthesis and characterization of the series [MTi(O-*i*-Pr)$_5$], M = Li, Na, and K, in solution and the solid state, including a single-crystal X-ray diffraction study of [LiTi(O-*i*-Pr)$_5$]$_2$.

Experimental Section

All manipulations were carried out under an atmosphere of dry (molecular sieves) and deoxygenated (MnO) dinitrogen.[9] All hydrocarbon and ethereal solvents were dried and distilled from sodium benzophenone ketyl. Alcohols were dried by distillation from magnesium turnings.[10] NMR solvents were dried over 4-Å molecular sieves and stored over N$_2$. Ti(NMe$_2$)$_4$ and Ti(O-*i*-Pr)$_4$ were prepared by the method of Bradley et al.[4a,11] 2-Propanol-*d*$_8$ was purchased from Aldrich Chemical Co. and dried prior to use. Elemental analyses were performed by Oneida Research Services. NMR data were recorded on a Bruker AC-250P NMR spectrometer by using the protio impurities of the deuterated solvents as reference for ^{1}H NMR and the ^{13}C resonance of the solvent as reference for ^{13}C NMR. Temperatures were calibrated with either ethylene glycol or methanol. Infrared spectra were recorded on Nicolet 6000 FTIR and Perkin-Elmer 1620 FTIR spectrophotometers. Mass spectra were recorded on a Finnegan GC–mass spectrometer. Molecular weights were determined cryoscopically by the freezing point depression of benzene.[12]

I. Synthesis of [LiTi(O-*i*-Pr)$_5$]. Ti(O-*i*-Pr)$_4$ (4.87 g; 17 mmol) was placed via syringe together with 40 mL of *n*-pentane in a 200-mL schlenk flask. A 40-mL aliquot of 2-propanol was added and the solution cooled to −78 °C. A 6.8-mL sample of 2.5 M *n*-butyllithium was added dropwise over about 15 min and a gas was evolved. A white fluffy precipitate was formed in a pale yellow solution. The solution was stirred and warmed to room temperature, whereupon the precipitate dissolved. After the solution was stirred for 1 h at room temperature, the volatile components were removed in vacuo to give a pale yellow solid. A minimum amount of *n*-pentane was added to dissolve the residue, and the sample was cooled to −30 °C for 12 h. During this time, large white crystals were formed. The solution was filtered at 0 °C and 3.51 g of solid analyzed as [LiTi(O-*i*-Pr)$_5$] was isolated: yield 58.9%. IR data (KBr disk, cm^{-1}): 2970 (m), 2925 (m), 2864 (m), 1463 (m), 1374 (s), 1361 (s), 1326 (m), 1172 (s, sh), 1162 (s, sh), 1126 (s), 1020 (s), 991 (s, sh), 978 (s), 962 (s, sh), 849 (m), 839 (m), 826 (m, sh), 714 (s), 708 (s, sh), 691 (s), 629 (s), 602 (s), 577 (s), 571 (m), 467 (m). ^{1}H NMR data (250 MHz, C$_6$D$_6$, 20 °C): 4.82 ppm, q, J_{H-H} = 6 Hz, 1 H, OC*H*Me$_2$; 1.38 ppm, d, 6 H, OCHMe$_2$. Variable-temperature ^{1}H NMR data (toluene-*d*$_8$): at 253 K, 4.85 ppm, br, 4 H, OC*H*Me$_2$; 4.68 ppm, br, 1 H, OC*H*Me$_2$; 1.60 ppm, br, 6 H, OCH*Me*$_2$; 1.34 ppm, br, 24 H, OCH*Me*$_2$, at 233 K, 4.85 ppm, septet, br, 4 H, OC*H*Me$_2$; 4.69 ppm, septet, 1 H, OC*H*Me$_2$; 1.64 ppm, d, *J* = 6 Hz, 6 H, OCH*Me*$_2$; 1.35 ppm, d, *J* = 6 Hz, 24 H, OCH*Me*$_2$; at 193 K, 4.78 ppm, M, br, 5 H, OC*H*Me$_2$; 1.70 ppm, d, *J* = 6 Hz, 6 H, OCH*Me*$_2$; 1.38 ppm, br, 24 H, OCHMe$_2$. ^{13}C{^{1}H} NMR data (62.9 MHz, toluene-*d*$_8$, 223 K): 70.1 ppm, s, OCHMe$_3$; ~73 ppm, v br, OCHMe$_2$; 27.4 ppm, s, br, OCH*Me*$_2$; 27.0 ppm, s, OCH*Me*$_2$. Mass spectral data (70 eV, 120 °C): major peaks (*m*/*e*) at 601, 1%; 535, 3%; 509, 4%; 468, 6%; 407, 6%; 403, 8%; 337, 6%; 283, 4%; 269, 100%; 225, 30%; 211, 15%; 205, 18%; 181, 15%; 167, 12%; 139, 30%; 112, 20%; 108, 20%; 99, 20%; 81, 30%; 73, 42%; 64, 22%; 43, 80%. Anal. Calcd for C$_{15}$H$_{35}$O$_5$LiTi: C, 51.3; H, 9.97. Found: C, 51.47; C, 51.35; H, 9.63; H, 10.14. The molecular weight was measured at two different concentrations, 0.025 and 0.040 M. The values were 692 ± 50 and 658 ± 28, respectively. The calculated value for [LiTi(O-*i*-Pr)$_5$]$_2$ was 702. Each value was determined by two measurements.

II. Synthesis of [NaTi(O-*i*-Pr)$_5$]. A 60% oil dispersion of NaH (5.12 g, 128 mmol) was placed into a 200-mL Schlenk flask and washed with two 50-mL portions of *n*-pentane. The solid was cooled to 0 °C, and a large excess (20 mL) of 2-propanol was slowly added (*Caution*! vigorous reaction!). After the reaction had subsided, the solution was warmed to room temperature, and the volatile components were removed in vacuo. The white solid obtained was taken up in *n*-pentane, the mixture filtered, and the solvent removed in vacuo. A standard *n*-pentane solution of NaO-*i*-Pr was prepared. Ti(O-*i*-Pr)$_4$ (20 g, 18.3 mmol) was placed in a 50-mL Schlenk flask, and 5 mL of the NaO-*i*-Pr solution containing 18.3 mmol was added dropwise at room temperature. During the addition, small colorless crystals appeared, and when the addition was complete, the solution was decanted and the crystals dried in vacuo to give 4.53 g, 12.4 mmol, of [NaTi(O-*i*-Pr)$_5$], a yield of 76.8%. IR data (KBr disk, cm^{-1}): 2967 (s), 2938 (m), 2875 (m), 1475 (m), 1388 (m), 1375 (m), 1337 (m), 1175 (m), 1125 (s), 1038 (s), 992 (s), 962 (s), 962 (s), 813 (m, sh), 800 (m), 706 (s), 625 (m), 600 (s), 556 (s), 462 (m). ^{1}H NMR data (250 MHz, C$_6$D$_6$, 20 °C): 4.50 ppm, q, J_{H-H} = 7 Hz, 1 H, OCHMe$_2$; 1.27 ppm, d, 6 H, OCHMe$_2$. Variable-temperature ^{1}H NMR data (toluene-*d*$_8$): at 233 K, 4.69 ppm, septet, br, *J* = 6 Hz, 1 H, OC*H*Me$_2$; 1.35 ppm, d, 6 H, OCH*Me*$_2$; at 193 K, 4.92 ppm, br, 1 H, OC*H*Me; 1.38 ppm, br, 6 H, OCH*Me*$_2$; at 173 K, 4.92 ppm, br, 4 H, OC*H*Me$_2$; 505 ppm, br, 1 H, OC*H*Me$_2$; 1.70 ppm, br, 6 H, OCH*Me*$_2$; 1.36 ppm, br, 24 H, OCH*Me*$_2$. ^{13}C{^{1}H} NMR data (62.9 MHz, toluene-*d*$_8$, 20 °C): 76.3 ppm, OCHMe$_2$; 26.8 ppm, OCH*Me*$_2$. Anal. Calcd for C$_{15}$H$_{35}$O$_5$NaTi: C, 49.17; H, 9.65. Found: C, 49.33; H, 9.08. The molecular weight of 699 ± 174 was measured at a concentration of 0.019 M. Attempts to measure the molecular weight at higher concentrations were hampered by the low solubility of this compound. The calculated value for [NaTi(O-*i*-Pr)$_5$]$_2$ was 732.

III. Synthesis of [KTi(O-*i*-Pr)$_5$]. KH dispersion in mineral oil was placed into a weighed flask, washed with pentane, filtered, dried in vacuo, and reweighed to give 0.94 g of dry KH. The KH was suspended in 75 mL of *n*-pentane and cooled to 0 °C, and an excess of 2-propanol was added slowly with rapid stirring. When the bubbling ceased and all the KH dissolved, the solution was warmed to room temperature, and the volatile components were removed under dynamic vacuum. A 100-mL

(4) (a) Bradley, D. C.; Mehrotra, R. C.; Gaur, P. D. *Metal Alkoxides*; Academic Press: London, 1978. (b) Mehrotra, R. C. Transition Metal Alkoxides. In *Advances in Inorganic Chemistry and Radiochemistry*; Eneleus, H. G., Sharpe, A. G., Eds.; Academic Press: London, 1983; Vol. 26, p 269. (c) Mehrotra, R. C.; Singh, J. *Inorg. Chem.* **1984**, *23*, 1046. (d) Mehrotra, R. C.; Agarwal, S. K. *Inorg. Chim. Acta* **1986**, *112*, 177. (e) Dubey, R. K.; Singh, A.; Mehrotra, R. C. *Inorg. Chim. Acta* **1986**, *118*, 151. (f) Govil, S.; Kapoor, P. N.; Mehrotra, R. C. *Inorg. Chim. Acta* **1975**, *15*, 43. (g) Bartley, W. G.; Wardlaw, W. *J. Chem. Soc.* **1958**, 422. (h) Bradley, D. C.; Caldwell, E. U.; Wardlaw, W. *J. Chem. Soc.* **1957**, 162.
(5) (a) Veith, M.; Rosler, R. *Z. Naturforsch.* **1986**, *41B*, 1071. (b) Veith, M.; Rosler, R. *Angew. Chem., Int. Ed. Engl.* **1982**, *21*, 858.
(6) Caulton, K. G. Private communication. Veith, M. *Chem. Rev.* **1990**, *90*, 3.
(7) Evans, W. J.; Deming, T. J.; Olofson, J. M.; Ziller, J. W. *Inorg. Chem.* **1989**, *28*, 4027.
(8) Hampden-Smith, M. J.; Smith, D. E.; Duesler, E. N. *Inorg. Chem.* **1989**, *28*, 3399.
(9) Shriver, D. F.; Drezden, M. A. *The Manipulation of Air-Sensitive Compounds*; 2nd ed.; Wiley-Interscience: New York, 1986; p 78.
(10) Burfield, D. R.; Smithers, R. H. *J. Org. Chem.* **1983**, *48*, 2420.
(11) Bradley, D. C.; Thomas, I. M. *J. Chem. Soc.* **1960**, 3857.
(12) Shoemaker, D. P.; Garland, C. W.; Steinfeld, J. I. *Experiments in Physical Chemistry*, 3rd ed.; McGraw-Hill Book Company: New York, 1974; pp 174–185.

Table I. Crystal Parameters for $[LiTi(O\text{-}i\text{-}Pr)_5]_2$

chemical formula: $C_{15}H_{35}O_5LiTi$	space group: $P2_1/n$ (No. 14)
fw = 702	T = 23 °C
a = 11.440 (8) Å	λ = 0.71073 Å
b = 16.396 (13) Å	ρ_{obsd} = 1.049 g/cm^3
c = 11.838 (8) Å	μ = 4.08 cm^{-1}
β = 92.59 (5) Å	transm coeff: 0.74–0.85
V = 2218.3 (3) Å^3	$R(F)$ = 9.36%
Z = 4	$R_w(F)$ = 10.28%

aliquot of n-pentane was added to the white solid, and 6.685 g (23.5 mmol) of $Ti(O\text{-}i\text{-}Pr)_4$ were added via syringe. No noticeable change was observed, and the colorless solution was stirred for 12 h. the volatile components were removed in vacuo, leaving a colorless residue to which toluene was added slowly until all the solid disappeared. The solution was cooled to −30 °C for 12 h, during which time large colorless crystals formed. The solution was filtered to give 3.729 g of solid. The solution was recooled to −30 °C to give a further crop of colorless crystals, 1.442 g. The combined isolated amount of solid obtained, which was analyzed as $[KTi(O\text{-}i\text{-}Pr)_5]$, was 5.171 g (13.5 mmol), a yield of 57.7%. IR data (KBr disk, cm^{-1}): 2967 (s), 2925 (m), 2859 (m), 1460 (m), 1370 (s), 1334 (m), 1323 (m), 1159 (s, sh), 1125 (s), 1011 (m, sh), 975 (s), 840 (s), 832 (s), 619 (s), 595 (s), 566 (s), 480 (m, sh), 463 (m), 440 (m). ^{1}H NMR data (250 MHz, C_6D_6, 20 °C): 4.97 ppm, q, J_{H-H} = 7 Hz, ^{1}H, $OCHMe_2$; 1.31 ppm, d, 6 H, $OCHMe_2$. Variable-temperature ^{1}H NMR data (toluene-d_8): no coalescence phenomena were observed when the sample was cooled to 183 K, but the resonances were broad at this temperature; 5.00 ppm, br, 1 H, OC*H*Me$_2$; 1.44 ppm, br, 6 H, OCH*Me*$_2$. ^{13}C NMR data (62.9 MHz, 20 °C, toluene-d_8): 72.7 ppm, O*C*HMe$_2$; 27.7 ppm, OCH*Me*$_2$. Anal. Calcd for $C_{15}H_{35}O_5KTi$: C, 47.10; H, 9.24. Found: C, 47.17; H, 9.105. The molecular weights of 795 ± 100 and 865 ± 66 were measured at concentrations of 0.024 M and 0.062 M, respectively. The calculated value $[KTi(O\text{-}i\text{-}Pr)_5]_2$ was 768. Each value was determined by two measurements.

IV. Reaction of Na with $Ti(O\text{-}i\text{-}Pr)_4$ and 2-Propanol. $Ti(O\text{-}i\text{-}Pr)_4$ (5.73 g, 20.2 mmol) was dissolved in 20 mL of 2-propanol. Sodium pieces (0.493 g, 20.6 mmol) were added, and the solution immediately became deep purple. The solution was refluxed for 3 h under dinitrogen and became deep purple brown (some of the sodium remained unreacted). When the reaction was cooled to room temperature, a white precipitate formed from a purple-brown solution. The 2-propanol was removed in vacuo, and pentane was added to give a white precipitate and a brown solution. The precipitate was filtered, washed with toluene, and dried in vacuo to give 2.19 g of solid. When the solution was left standing at room temperature, a white solid precipitated from the brown-purple solution, which upon drying in vacuo gave 1.01 g of white purple solid. ^{1}H NMR data (250 MHz, C_6D_6, 20 °C); 4.92 ppm, q, J_{H-H} = 7 Hz, 1 H, $OCHMe_2$; 4.76 ppm, q, J_{H-H} = 7 Hz, 1 H, $OCHMe_2$; 1.36 ppm, d, 6 H, $OCHMe_2$; 1.13 ppm, d, 6 H, $OCHMe_2$. Anal. Found: C, 47.93; H, 9.63.

V. Synthesis of $[LiTi(O\text{-}i\text{-}Pr\text{-}d_7)_5]$. $Ti(O\text{-}i\text{-}Pr\text{-}d_7)_4$ was prepared by the addition of 5 equiv of DO-i-Pr-d_7 to $Ti(NMe_2)_4$ in n-pentane. The product was distilled in vacuo. LiO-i-Pr-d_7 was prepared by the addition of n-BuLi to DO-i-Pr-d_7 at −78 °C and was added to $Ti(O\text{-}i\text{-}Pr\text{-}d_7)_4$ as described above. The infrared data for both $Ti(O\text{-}i\text{-}Pr)_4$ and $Ti(O\text{-}i\text{-}Pr)_4$ and $Ti(O\text{-}i\text{-}Pr\text{-}d_7)_4$ are reported below in detail for comparative purposes (see text). $Ti(O\text{-}i\text{-}Pr)_4$ IR data (pure liquid, cm^{-1}): 2945 (s), 2925 (m), 2875 (m), 1463 (m), 1450 (m), 1375 (m), 1363 (m), 1325 (m), 1162 (s, sh), 1125 (s, br), 1000 (s, br), 938 (m), 850 (s), 825 (m), 619 (s, br), 563 (m), 513 (m), 450 (m). $Ti(O\text{-}i\text{-}Pr\text{-}d_7)_4$ IR data (pure liquid, cm^{-1}): 2225 (s), 2125 (m), 2100 (m), 2075 (m), 1263 (m), 1213 (s), 1163 (s), 1150 (s), 1088 (s), 1050 (s), 1025 (s), 987 (s), 900 (m), 830 (s), 788 (m), 725 (s), 575 (s, br). ^{2}H NMR data for $Ti(O\text{-}i\text{-}Pr\text{-}d_7)_4$ (38.4 MHz, C_6H_6, 20 °C): 4.42 ppm, s, br, 1 D, OC*D*(CD$_3$)$_2$; 1.15 ppm, s, br, 6 D, OCD (C*D*$_3$). ^{13}C NMR data for $Ti(O\text{-}i\text{-}Pr\text{-}d_7)_4$ (62.9 MHz, C_6H_6, 20 °C): 75.1 ppm, t, J_{C-D} = 24 Hz, O*C*D(CD$_3$)$_2$, 25.1 ppm, septet, J_{C-D} = 19 Hz, OCD (*C*D$_3$)$_2$. IR data for $LiTi(O\text{-}i\text{-}Pr\text{-}d_7)_5$ (KBr Disk, cm^{-1}): 2350 (m), 2225 (s), 2163 (m), 2100 (m), 1213 (m), 1175 (m, sh), 1150 (s), 1100 (m, sh), 1075 (s), 1050 (s), 1024 (m), 1013 (m), 975 (m, sh), 950 (m), 850 (s), 775 (s), 575 (m, sh), 550 (s), 524 (m).

VI. X-ray Crystal Structure of $LiTi(O\text{-}i\text{-}Pr)_5$. Gray-white crystals of $[LiTi(O\text{-}i\text{-}Pr)_5]_2$ (**1**) suitable for X-ray structure determination were grown from pentane and mounted, under dinitrogen, in a capillary. All specimens examined diffracted diffusely.

In Table I, crystal data collection and refinement parameters are collected. The determination of the space group was unambiguous ($P2_1/n$: $0k0$, $k = 2n + 1$; $h0l$, $h + l = 2n + 1$). An empirical correction for absorption was applied to the data set (216 Ψ-scan reflections, pseudoellipsoid model, T_{max}/T_{min} = 1.289). The structure was solved by direct methods, which located the Ti atom. The remaining non-hydrogen atoms were located through subsequent least-squares cycles and difference Fourier calculations. All non-hydrogen atoms were refined anisotropically, and hydrogen atoms were included as idealized isotropic contributions (d(CH) = 0.960 Å, $U = 1.2U$ for attached C). All software and the source of the scattering factors are contained in the SHELXTL program library (G. Sheldrick, Nicolet Corp., Madison, WI).

Atom coordinates are given in Table II, and selected bond distances and angles are collected in Table III. Additional crystallographic data are available as supplementary material.

Table II. Atomic Coordinates (×10^4) and Isotropic Thermal Parameters (Å^2 × 10^3)

	x	y	z	U,^{a} Å^2
Ti	327.9 (20)	8689.3 (13)	1150.0 (19)	75.8 (9)
Li	1154 (18)	10034 (14)	−183 (18)	84 (9)
O(1)	−1147 (7)	9176 (5)	1390 (7)	85 (4)
O(2)	1731 (6)	9262 (5)	938 (7)	92 (4)
O(3)	283 (8)	7654 (5)	693 (8)	113 (4)
O(4)	656 (8)	8494 (6)	2652 (7)	113 (5)
O(5)	−31 (6)	9155 (5)	−377 (6)	71 (3)
C(1)	−1919 (15)	9017 (11)	2212 (15)	121 (8)
C(2)	−2667 (27)	8396 (16)	1906 (27)	428 (31)
C(3)	−2612 (19)	9666 (15)	2520 (19)	248 (17)
C(4)	2816 (17)	9147 (14)	1476 (18)	163 (11)
C(5)	3568 (17)	9819 (14)	1346 (22)	324 (22)
C(6)	3482 (19)	8547 (13)	1043 (27)	345 (26)
C(7)	460 (20)	6874 (10)	1113 (15)	153 (10)
C(8)	1297 (23)	6474 (11)	589 (20)	254 (18)
C(9)	−418 (26)	6378 (13)	910 (32)	497 (39)
C(10)	862 (23)	8488 (14)	3800 (12)	226 (15)
C(11)	1100 (24)	9136 (16)	4338 (16)	316 (22)
C(12)	580 (26)	7848 (16)	4368 (18)	306 (21)
C(13)	−203 (19)	8732 (15)	−1358 (18)	163 (12)
C(14)	871 (22)	8408 (11)	−1844 (18)	251 (17)
C(15)	−1297 (26)	8473 (14)	−1557 (21)	264 (20)

^{a} Equivalent isotropic U defined as one-third of the trace of the orthogonalized U_{ij} tensor.

Table III. Selected Bond Distances and Angles for $[LiTi(O\text{-}i\text{-}Pr)_5]_2$

(a) Bond Distances (Å)			
Ti–O(1)	1.900 (9)	Ti–O(4)	1.829 (9)
Ti–O(2)	1.886 (8)	Ti–O(5)	1.988 (8)
Ti–O(3)	1.782 (9)	Li–O(2)	1.930 (23)
Li–O(5)	1.984 (23)	Li–O(1a)	1.928 (23)
Li–O(5a)	1.982 (23)	O(2)–C(4)	1.382 (20)
O(1)–C(1)	1.367 (20)	O(4)–C(10)	1.368 (16)
O(3)–C(7)	1.383 (19)	Ti···Li	2.895 (22)
O(5)–C(13)	1.360 (23)	Ti···Li(a)	2.896 (21)
Li···Li(a)	2.697 (41)		
(b) Bond Angles (deg)			
O(1)–Ti–O(2)	125.3 (4)	O(2)–Ti–O(3)	116.5 (4)
O(1)–Ti–O(3)	115.6 (4)	O(1)–Ti–O(4)	94.1 (4)
O(2)–Ti–O(4)	94.5 (4)	O(3)–Ti–O(4)	97.5 (4)
O(2)–Ti–O(5)	80.2 (3)	O(1)–Ti–O(5)	80.0 (3)
O(4)–Ti–O(5)	167.4 (4)	O(3)–Ti–O(5)	95.1 (4)
O(2)–Li–O(1a)	160.1 (12)	O(2)–Li–O(5)	79.3 (9)
O(5)–Li–O(5a)	94.3 (9)	O(5)–Li–O(1a)	115.0 (10)
Ti–O(1)–C(1)	129.3 (9)	O(2)–Li–O(5a)	114.6 (11)
C(1)–O(1)–Li(a)	132.4 (11)	O(1A)–Li–O(5a)	79.4 (9)
Ti–O(2)–C(4)	128.6 (11)	Ti–O(1)–Li(a)	98.3 (7)
Ti–O(3)–C(7)	140.3 (10)	Ti–O(2)–Li	98.7 (7)
Ti–O(5)–Li	93.6 (7)	Li–O(2)–C(4)	132.7 (12)
Li–O(5)–C(13)	122.8 (12)	Ti–O(4)–C(10)	170.2 (12)
Li–O(5)–Li(a)	85.7 (9)	Ti–O(5)–C(13)	126.6 (11)
C(13)–O(5)–Li(a)	123.8 (12)	Ti–O(5)–Li(a)	93.7 (7)

Results and Discussion

Upon following a previously published procedure[13] for the preparation of $NaTi(O\text{-}i\text{-}Pr)_5$ involving the reaction of sodium metal with 2-propanol solutions of $Ti(O\text{-}i\text{-}Pr)_4$, we observed the immediate formation of a purple solution probably corresponding to the reduction of Ti(IV) to Ti(III). This color change was not previously reported and may only correspond to a small amount of reduction to an intensely colored material. A white solid was

(13) Mehrotra, R. C.; Agarwal, M. M. *J. Chem. Soc. A* **1967**, 1026.

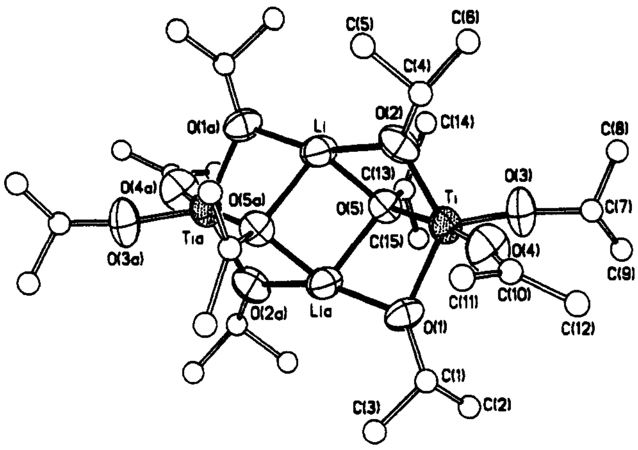

Figure 1. ORTEP plot of [LiTi(O-*i*-Pr)$_5$]$_2$ showing the atom numbering schemes. Thermal ellipsoids are at 30%.

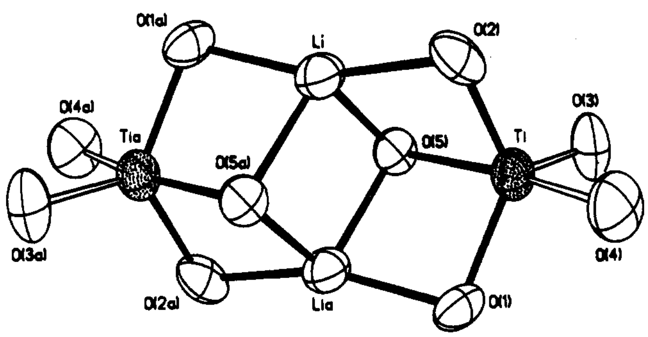

Figure 2. View of the Li, O, and Ti core of [LiTi(O-*i*-Pr)$_5$]$_2$.

isolated from this reaction, but it did not analyze correctly for [LiTi(O-*i*-Pr)$_5$]. The analytical data for the isolated material are consistent with an empirical formula somewhere between [Ti$_2$(O-*i*-Pr)$_6$)O] (46.2% C and 9.0% H) and [Ti$_4$(O-*i*-Pr)$_{14}$O] (48.9% C and 8.7% H). The analysis is close to that reported for [Ti$_4$(O-*i*-Pr)$_{12}$O], but the color of the solid is not consistent with the presence of Ti(III).[14] Reduction of Ti(O-*i*-Pr)$_4$ with an excess of $LiBH_4$ has been reported under mild conditions and yields a purple, mixed-valence Ti(III)/Ti(IV) oxo–alkoxide.[14]

As an alternative to the above procedure, we found that [MTi(O-*i*-Pr)$_5$] can be prepared by the reaction of preformed alkali-metal isopropoxide compounds with Ti(O-*i*-Pr)$_4$, according to eq 1. Spectroscopic data indicated that these reactions are

$$\text{M(O-}i\text{-Pr)} + \text{Ti(O-}i\text{-Pr)}_4 \rightarrow [\text{MTi(O-}i\text{-Pr)}_5] \quad (1)$$

quantitative, but the isolated crystalline yields are in the region of 57–77%.

I. Solid-State Structure of [LiTi(O-*i*-Pr)$_5$]$_2$. LiTi(O-*i*-Pr)$_5$ is dimeric in the solid state and possesses C_i molecular symmetry. Figure 1 shows an ORTEP view of this molecule with the atom numbering scheme, and Figure 2 emphasizes the coordination environment of the metal atom core. The molecule consists of two distorted-trigonal-bipyramidal Ti(IV) centers joined by lithium bridges. The titanium center possesses two terminal, two μ_2-bridging alkoxide groups, and one μ_3-bridging alkoxide ligand. The degree of bridging of the alkoxide groups is paralleled by the Ti–O bond lengths where terminal Ti–O(3) (1.782 (9) Å) and terminal Ti–O(4) (1.829 (9) Å) < μ_2-Ti–O(2) (1.886 (8) Å) and μ_2-Ti–O(1) (1.900 (9) Å) < μ_3-Ti–O(5) (1.988 (8) Å), analogous to data obtained for [Ti(OMe)$_4$]$_4$.[15] The trigonal-bipyramidal coordination environment about Ti is distorted by an opening of the O(2)–Ti–O(1) angle (125.3 (4)°) and a reduction in the O(4)–Ti–O(3) angle (167.4 (4)°) probably as a combined result of the steric demands of the alkoxide ligands and the geometric constraints of the coordination environment about Li. The angle at the oxygen atom of the terminal axial alkoxide (Ti–O(4)–C(10) ~ 170°) is significantly more linear than that of the equatorial terminal alkoxide Ti–O(3)–C(7) (~140°) possibly as a result of better overlap between the oxygen lone pairs and the e″ set of vacant Ti d orbitals.[16] The lithium coordination environment is analogous to that observed previously for LiSn(O-*t*-Bu)$_3$.[5a] The central metal–oxygen atom core of [LiTi(O-*i*-Pr)$_5$]$_2$ is analogous to that of MSn(O-*t*-Bu)$_3$ (M = Li, Na) with the addition of two terminal alkoxides at each titanium and is also analogous to the structures of W$_4$(OEt)$_{16}$[17] and Ti$_4$(OMe)$_{16}$.[16] Another way to view this core is as two distorted face-sharing cubes, each with one vertex missing from opposite corners.[18] A similar framework has also been observed in [Tl$_2$Sn(OEt)$_6$]$_\infty$.[8]

II. Solid-State and Solution Spectroscopic Data. In benzene and toluene solution, [MTi(O-*i*-Pr)$_5$], M = Li, Na, and K, exhibit only a single time-averaged type of isopropoxide ligand environment at room temperature as determined by ^{1}H NMR and ^{13}C spectroscopy. However, as toluene solutions are cooled, the ^{1}H NMR signals broaden and decoalesce. For [LiTi(O-*i*-Pr)$_5$], two types of isopropoxide ligand environments are clearly observed in a 4:1 ratio at −20 °C, with a coalescence temperature for this process of 0 °C. As the solution is cooled further, the resonances due to the isopropoxide ligand of relative intensity 4 broaden, while those of intensity 1 remain relatively sharp. As a result, we believe there may be another fluxional process that is rapid at −80 °C that could not be "frozen out", even upon cooling [LiTi(O-*i*-Pr)$_5$] to −120 °C in a 60:40 freon-12–toluene-d_8 solution. [NaTi(O-*i*-Pr)$_5$] exhibits similar temperature-dependent ^{1}H NMR spectra, but the coalescence temperature is much lower (−80 °C) compared to that of the Li analogue. The ^{1}H NMR resonances of the isopropoxide ligands of the potassium analogue remained sharp upon cooling to −70 °C and started to broaden at −90 °C, but the solution could not be cooled to a temperature low enough (minimum T = −90 °C) to observe coalescence. While the total number of different types of alkoxide ligands in the low-temperature spectra of lithium and sodium species is consistent with the empirical formula [MTi(O-*i*-Pr)$_5$], its correspondence with the solid-state structural data for [LiTi(O-*i*-Pr)$_5$]$_2$ is not unambiguously established. If the terminal and μ_2-O-*i*-Pr ligands exchange with one another, but not with the μ_3-O-*i*-Pr ligand, the observed 4:1 pattern would result. However, a cryoscopic molecular weight determination indicated that the lithium analogue was dimeric at ~+5 °C, close to the coalescence temperature for the solution dynamic process. This observation is consistent with an intramolecular solution dynamic process and is corroborated by the fact that a similar value for the molecular weight of [LiTi(O-*i*-Pr)$_5$] was obtained at different concentrations. The low-temperature ^{1}H NMR data for [LiTi(O-*i*-Pr)$_5$] were measured on two different occasions with solutions of different concentrations, and a similar coalescence temperature was observed. This is also consistent with an intramolecular process. However, it must be noted that trace amounts of alcohol that may be present at levels below the limits of NMR detection may undergo rapid exchange with alkoxide ligands and complicate the situation. An intramolecular dynamic process is not surprising based on the well-known stereochemical nonrigidity of five-coordinate metal centers. Cryoscopic molecular weight determinations for the sodium and potassium species also are consistent with the presence of a dimeric unit in benzene solution. In contrast, both [MTi(O-*i*-Pr)$_5$] compounds, M = Li and Na, have previously been found to be monomeric in ether and 2-propanol solutions, respectively.[13] Unfortunately, ^{13}C NMR data provided no further insight since only two types of isopropoxide ligands were observed

(14) Sabo, S.; Choukroun, R.; Gervais, D. *J. Chem. Soc., Dalton Trans.* **1981**, 2328.
(15) (a) Wright, D. A.; Williams, D. A. *Acta Crystallogr.* **1968**, *B24*, 1107. (b) Ibers, J. A. *Nature* **1963**, *197*, 686.
(16) Rossi, A. R.; Hoffmann, R. *Inorg. Chem.* **1975**, *14*, 365.
(17) Chisholm, M. H.; Huffman, J. C.; Kirkpatrick, C. C.; Leonelli, J., Folting, K. *J. Am. Chem. Soc.* **1981**, *103*, 6093.
(18) Holmes, R. R.; Day, R. O.; Chandrasekhar, V.; Schmid, C. G.; Swamy, K. C.; Holmes, J. M. *Inorganic and Organometallic Polymers*; Zeldin, M., Wynn, K. J., Allcock, H. R., Eds.; ACS Symposium Series 360; American Chemical Society: Washington, DC, 1988. Konnick, W. D.; Zuckerman, J. J. *Inorg. Chem.* **1976**, *12*, 3034.

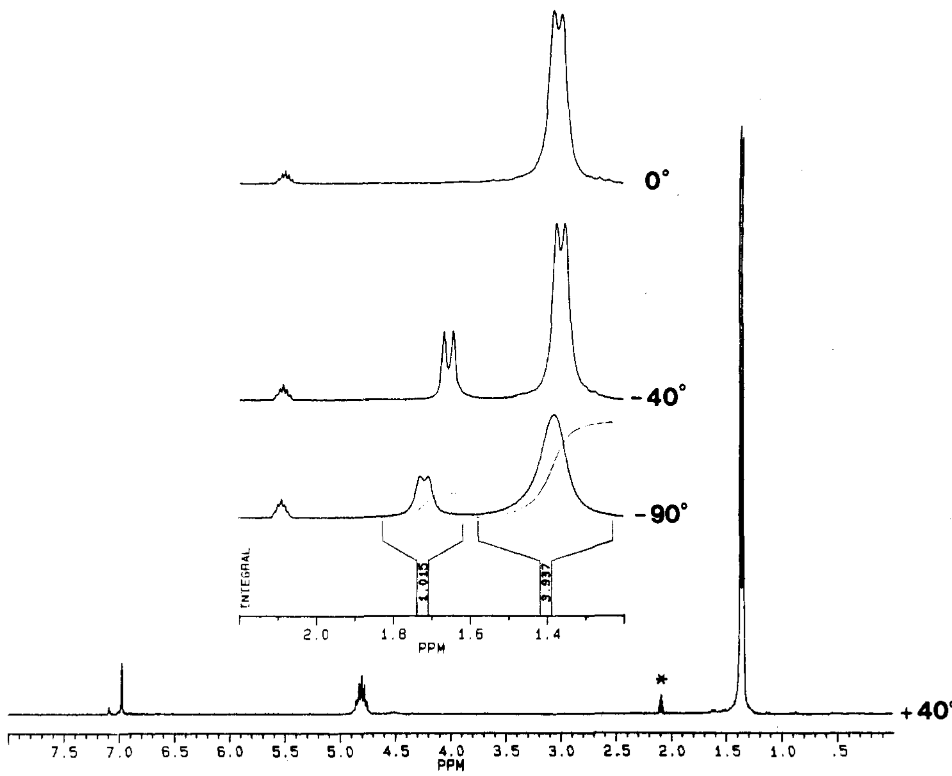

Figure 3. Variable-temperature ^{1}H NMR spectra of $[LiTi(O\text{-}i\text{-}Pr)_5]_2$ in toluene-d_8 solution. An asterisk marks the protio impurity due to the solvent.

for $[LiTi(O\text{-}i\text{-}Pr)_5]$ in a 1:4 ratio, consistent with the ^{1}H NMR spectroscopic data.

In the mass spectrum of crystalline $[LiTi(O\text{-}i\text{-}Pr)_5]_2$, a molecular ion for the dimeric unit is not observed, but a mass consistent with the loss of a methyl group from the monomer is observed at $m/e = 333$. The spectrum is dominated by fragmentation of titanium isopropoxide species, and the base mass of $m/e = 269$ corresponds to $Ti(O\text{-}i\text{-}Pr)_3(OCHMe)^+$.

The solid-state IR spectra of the title compounds were examined to determine whether or not the lithium, sodium, and potassium analogues possessed a similar structure in the solid state. The IR spectra of group 4 metal *tert*-butoxide and metal isopropoxide species have previously been analyzed in some detail and some ν(Ti–O) stretching frequencies have been tentatively assigned.[19] For example, ν(Ti–O) in $Ti(O\text{-}i\text{-}Pr)_4$ has been assigned to the band at 619 cm^{-1}, and we have observed a band at 599 cm^{-1} in $Ti(O\text{-}t\text{-}Bu)_4$ that we ascribe to ν(Ti–O) by comparison with the IR data for $Sn(O\text{-}t\text{-}Bu)_4$ and $Sn(O\text{-}t\text{-}Bu\text{-}d_9)_4$.[20] To confirm the assignment of ν(Ti–O) in $Ti(O\text{-}i\text{-}Pr)_4$, we prepared $Ti(O\text{-}i\text{-}Pr\text{-}d_7)_4$ and compared their liquid-phase IR spectra. In $Ti(O\text{-}i\text{-}Pr\text{-}d_7)_4$, the band at 619 cm^{-1} disappeared and a new strong band appeared at 563 cm^{-1} where the difference in metal–oxygen stretching frequencies, ν(Ti–O-*i*-Pr) – ν(Ti–O-*i*-Pr-d_7), defined here as $\Delta\nu$(Ti-O), is 56 cm^{-1}. This value is at somewhat lower energy than that predicted[21] by using a simplified "diatomic molecule" approach and assuming that –O-*i*-Pr and –O-*i*-Pr-d_7 ligands are point masses of 59 and 66 mass units, respectively. In the solid state (KBr disk), the IR spectra of $[MTi(O\text{-}i\text{-}Pr)_5]$, M = Li, Na, and K, are very similar; furthermore, it is noteworthy that, in all three compounds and in $Ti(O\text{-}i\text{-}Pr)_4$ (in solution), the bands observed between 3000 and 800 cm^{-1} occur at similar positions and intensities. These bands have also been observed in other metal isopropoxide compounds and have been assigned.[19a] The bands in the region of 600 cm^{-1} are therefore probably due to ν(M–O) stretches and, in principle, should be characteristic for each of the lithium, sodium, and potassium compounds. To test this assignment, $[LiTi(O\text{-}i\text{-}Pr\text{-}d_7)_5]$ was prepared and the solid-state IR spectrum compared with that of the protio analogue. With use of a method similar to that discussed above, the calculated position of ν(Ti–O-*i*-Pr-d_9) in the deuterated analogue is expected to be centered at 586 cm^{-1} (using an average ν(Ti–O-*i*-Pr) value of 601 cm^{-1} for $[LiTi(O\text{–}i\text{-}Pr)_5]_2$). The new large band observed in the ν(M–O) region for $[LiTi(O\text{–}i\text{-}Pr\text{-}d_7)_5]$ is centered at 552 cm^{-1}, which does not correspond very well to the calculated value but does correspond quite well to the value of 545 cm^{-1} predicted from the observed difference of $\Delta\nu$(Ti–O) = 56 cm^{-1} obtained for the protio and deuterio $[Ti(O\text{–}i\text{-}Pr)_4]$ compounds. On the basis of these data, we assign the metal–oxygen stretching frequencies (cm^{-1}) for the title compounds in the solid state as follows: $[LiTi(O\text{-}i\text{-}Pr)_5]$, 632, 602, 577; $[NaTi(O\text{–}i\text{-}Pr)_5]$, 625, 600, 556; $[KTi(O\text{–}i\text{-}Pr)_5]$, 619, 595, 566. It is tempting to assign the three bands observed in each case to the three types of alkoxide ligand (terminal and μ^2- and μ^3-bridging) observed in the solid-state structure of $[LiTi(O\text{–}i\text{-}Pr)_5]_2$ and to use this as evidence that all three compounds are isostructural. Further studies are required, however, to confirm such speculation, especially in light of the literature data, which indicate that, for a series of complexes $MM'(OR)_n$ where M′ is constant and M is various alkali metals, a change in structure in the solid state is observed at M = potassium upon descending group 1.[5a]

Conclusions

The series $[MTi(O\text{-}i\text{-}Pr)_5]$, M = Li, Na, and K, has been prepared by the reaction of alkali-metal isopropoxides with titanium isopropoxide and was crystallized in reasonable yields. While $[LiTi(O\text{-}i\text{-}Pr)_5]$ is unambiguously dimeric in the solid state and in benzene solution, the sodium and potassium analogues appear dimeric in solution, but the degree of oligomerization in the solid state could not conclusively be established based on comparison of the solid-state IR data. In benzene and toluene solution at room temperature, all the title compounds undergo a rapid dynamic exchange process on the ^{1}H NMR time scale, but their dimeric nature is probably maintained. Further work to determine unambiguously the solution structure of these and other metal alkoxides is essential to a complete understanding of their subsequent

(19) (a) Lynch, C. T.; Mazdiyasni, K. S.; Smith, J. S.; Crawford, W. J. *Anal. Chem.* **1964**, *36*, 2333. (b) Sheppard, N. *Trans. Faraday Soc.* **1950**, *46*, 533. (c) Seubold, F. H. *J. Org. Chem.* **1956**, *21*, 157. (d) Ory, H. A. *Anal. Chem.* **1960**, *32*, 509.

(20) Hampden-Smith, M. J.; Wark, T. A.; Rheingold, A.; Huffmann, J. C. *Can. J. Chem.*, in press.

(21) Bradley, D. C.; Westlake, A. H. In *Proceedings of the Symposium on Coordination Chemistry, Tihany, Hungary*; Hungarian Academy of Science: Budapest, 1965; p 309 (referred to in ref 4a).

hydrolytic condensation. To this end, a criterion has been devised for establishing the position of ν(Ti–O) stretching frequencies in titanium(IV) isopropoxide compounds by determining the difference ν(Ti–O-*i*-Pr) – ν(Ti–O-*i*-Pr-d_7), defined here as $\Delta\nu$(Ti–O-*i*-Pr) = 57 cm^{-1}. We envisage that this may be utilized in other systems as a means of unambiguously establishing the position of ν(M–O) stretching frequencies and may aid characterization of metal alkoxide compounds in solution.[22]

During submission of this manuscript, we learned that the single-crystal X-ray diffraction structure of NaTi(O-*i*-Pr)$_5$ was solved on crystals grown from pentane solution at –25 °C. The structure (R = 8.6%) consists of infinite linear chains of alternating tetrahedral sodium and distorted-trigonal-bipyramidal titanium atoms connected by bridging isoproxy groups.[23]

Acknowledgment. We thank Drs. Dan Doughty and Chuck Peden for helpful discussions, Eva Quesnell for typing the manuscript, and the NSF for purchase of an NMR spectrometer under the Chemical Instrumentation Program. This work was financially supported by Sandia National Laboratories, Contract No. 05-2694.

Supplementary Material Available: A full listing of bond lengths and angles, anisotropic thermal parameters, H-atom coordinates, and crystal data (4 pages); a listing of observed and calculated structure factors (7 pages). Ordering information is given on any current masthead page.

(22) ^{13}C NMR data have also been used to examine the solution structures of titanium alkoxide compounds: Holloway, C. E. *J. Chem. Soc., Dalton Trans.* **1976**, 1050.

(23) Bradley, D. C.; Patel, A. Private communication, June 1990.

Contribution from the Institut für Anorganische und Physikalische Chemie, Universität Bern, CH-3000 Bern 9, Switzerland, Laboratorium für Neutronenstreuung, ETHZ, 5303 Würenlingen, Switzerland, and Institut Laue Langevin, 38042 Grenoble Cedex, France

Exchange Interactions in Rare-Earth-Metal Dimers. Neutron Spectroscopy of $Cs_3Yb_2Cl_9$ and $Cs_3Yb_2Br_9$

Hans U. Güdel,*[,1a] Albert Furrer,[1b] and Herma Blank[1c]

Received March 8, 1990

The title compounds were synthesized and studied by high-resolution inelastic neutron scattering. Magnetic dimer excitations were measured on polycrystalline samples at 1.8 K. The observed energy splittings of the ground state can be accounted for by a Heisenberg Hamiltonian with antiferromagnetic exchange parameters $2J$ = –3.25 (3) and –2.87 (3) cm^{-1} for $Cs_3Yb_2Cl_9$ and $Cs_3Yb_2Br_9$, respectively.

1. Introduction

A great deal of work has been done toward a better understanding of exchange interactions in dimers of transition-metal ions.[2] In contrast, dimers of rare earth (RE) metal ions have received much less attention, and little is known to date about the nature of magnetic couplings in such species.[3–7] Due to the shielding of magnetic 4f electrons, as compared to 3d electrons in transition metal ion systems, exchange interactions are expected to be considerably smaller in rare-earth-metal systems. This is confirmed by magnetic ordering temperatures below 5 K in rare-earth-metal halides. In addition to exchange interactions, magnetic dipole–dipole interactions are considered to play a crucial role in these magnetic ordering phenomena. Highly anisotropic g values are characteristic of most rare-earth-metal ions in noncubic crystalline environments, and correspondingly, exchange interactions are often represented by Ising or XY operators.[8,9]

It is not a priori clear whether the same effective Hamiltonians can also be used to describe the energetic splittings resulting from exchange interactions in dimers. A Heisenberg Hamiltonian has been found adequate for an interpretation of EPR results obtained for Gd^{3+} dimers in a variety of host lattices.[4,10] This is a special case, however, since the Gd^{3+} ion, with its half-filled 4f shell, has a completely isotropic ground-state $^8S_{7/2}$. On the other hand, evidence of anisotropic exchange as well as contributions from magnetic dipole–dipole interactions was obtained from EPR measurements of Ce^{3+} and Nd^{3+} dimers.[3] The interaction parameters were obtained from the experimental data by rather involved procedures in these investigations.

From a study of a number of transition-metal dimers we have found that inelastic neutron scattering (INS) is a very straightforward technique for the determination of exchange parameters.[11] Transitions between exchange-split components of the ground state are usually observable. These energy splittings can thus be determined in a very direct way, without any complicating effects from external magnetic fields as in EPR or magnetic susceptibility measurements. The INS technique should be equally useful for the study of rare-earth-metal dimers,[12] and we chose the family of compounds with composition $Cs_3(RE)_2Br_9$ (RE = Tb^{3+}, Dy^{3+}, Ho^{3+}, Er^{3+}, Yb^{3+}) for our studies. These compounds all crystallize in space group $R\bar{3}c$, and they contain the dimeric species $(RE)_2Br_9^{3-}$ depicted in Figure 1. The great advantage of such a system compared to one doped with RE ions is the presence of only one magnetic species and thus the absence of overlapping spectra. First results of these studies are reported in refs 12–16. They show that for RE = Tb^{3+}, Dy^{3+}, and Yb^{3+} a Heisenberg model adequately describes the observed splittings as long as only

* To whom correspondence should be addressed.

(1) (a) Universität Bern. (b) ETHZ. (c) Institut Laue Langevin.
(2) *Magneto-Structural Correlations in Exchange Coupled Systems*; Willett, R. D., Gattschi, D., Kahn, O., Eds.; D. Reidel: Dordrecht, The Netherlands, 1985.
(3) Riley, J. D.; Baker, J. M.; Birgenau, R. J. *Proc. R. Soc. London* **1970**, *A320*, 369.
(4) Cochrane, R. W.; Wu, C. Y.; Wolf, W. P. *Phys. Rev. B* **1973**, *8*, 4348.
(5) Wolf, W. P. *J. Phys.* **1971**, *C1*, 26.
(6) Velter-Stefanescu, M.; Nislor, S. V. *Phys. Rev. B* **1986**, *34*, 1459.
(7) Maedra, A.; Sugimoto, H. *J. Chem. Soc., Faraday Trans. 2* **1986**, *82*, 2019.
(8) De Jongh, L. J.; Miedema, A. R. *Adv. Phys.* **1974**, *23*, 1.
(9) Carlin, R. L. *Magnetochemistry*; Springer: Berlin, 1986.
(10) Cochrane, R. W.; Wolf, W. P. *Solid State Commun.* **1971**, *9*, 1997 and refs 2–5 therein.
(11) Güdel, H. U.; Furrer, A.; Kjems, J. K. *J. Magn. Magn. Mater.* **1986**, 54–57, 1453 and references therein.
(12) Furrer, A.; Güdel, H. U.; Darriet, J. *J. Less-Common Met.* **1985**, *111*, 223.
(13) Dönni, A.; Furrer, A.; Blank, H.; Heidemann, A.; Güdel, H. U. *J. Phys.* **1988**, *C8*, 1513.
(14) Dönni, A.; Furrer, A.; Blank, H.; Heidemann, A.; Güdel, H. U. *Physica B* **1989**, *156 + 157*, 370.
(15) Furrer, A.; Güdel, H. U.; Blank, H.; Heidemann, A. *Phys. Rev. Lett.* **1989**, *62*, 210.
(16) Furrer, A.; Güdel, H. U.; Krausz, E. R.; Blank, H. *Phys. Rev. Lett.* **1990**, *64*, 68.

0020-1669/90/1329-4081$02.50/0